Multivariable controller for stationary flat plate solar collectors *

Andrea Tosi[1], Lidia Roca[2], Juan D. Gil[3], Antonio Visioli[1] and Manuel Berenguel[3]

***Abstract*— The water flow rate control, which is the principal control loop required to operate stationary solar fields, can be as simple as designing a PID controller for a unique pump whose behavior can be approximated by a first-order system with delay. Nevertheless, when the water flow rate is manipulated with multiple actuators (pumps or valves), the problem presents some challenges due to hydraulic interactions. This paper presents a multivariable controller scheme to deal with the control of a solar field with five pumping systems. Simulation and experimental results are included to demonstrate the effectiveness of the proposed controller.**

I. INTRODUCTION

From the control point of view, stationary flat plate solar collectors require fewer control loops than parabolic through collectors because the solar collector movement is not a degree of freedom. For this reason, the first variable that must be controlled in this kind of systems is the heat transfer fluid (HTF) flow rate, whose variations affect to the outlet temperature of the solar field [3]. Therefore, to maintain the desired outlet temperature despite the variability in the operating conditions (such as the solar irradiance level), the first control engineering work must be the design of the HTF flow rate controller. Usually, this control design is a simple stage because the solar fields are designed to assure similar flow rates in all the loops and they have only a main pumping system whose dynamics can be approximated by a first or second order system with delay [4]. Nevertheless, some new designs of solar collector systems, such as the one presented in this paper, require a pumping system for each loop. In these cases, the complexity of the HTF flow rate control loop is higher because the variations in the pumping system of one loop affect not only that loop, but also the other loops. For large solar fields, the use of independent controllers for the flow rates can improve the response of the temperature controllers because the irradiance level can be different in different parts of the solar field due to passing clouds. Last studies related with appropriate controllers considering multiple control variables, such as [6], [8], do not consider the hydraulic system as a MIMO system with coupling. This paper demonstrates the importance of considering the hydraulic interaction inside the design of the temperature control strategy and it is organized as follows. Section 2 describes the experimental facility under study. In Section 3, the hydraulic model is presented and the results are compared with data from the facility. Section 4 describes the multivariable controller proposed and simulation and experimental results are included in Section 5. Conclusions are discussed in Section 6.

*This project has received funding from the European Union's Horizon 2020 research and innovation programme under grant agreement No 731287. This work has been also funded by the National R+D+i Plan Projects DPI2014-56364-C2-1/2-R and DPI2017-85007-R of the Spanish Ministry of Economy, Industry and Competitiveness and ERDF funds.

[1]Andrea Tosi and Antonio Visioli are with the Dipartimento di Ingegneria Meccanica e Industriale, University of Brescia - Italy, a.tosi007@studenti.unibs.it, antonio.visioli@unibs.it

[2]Lidia Roca is with CIEMAT-Plataforma Solar de Almería, Ctra. de Senés s/n, Tabernas, 04200 Almería, Spain, lidia.roca@psa.es

[3]Juan D. Gil an Manuel Berenguel are with Centro Mixto CIESOL, ceiA3, Universidad de Almería, Ctra. Sacramento s/n, Almería 04120, Spain, {juandiego.gil,beren}@ual.es

II. SYSTEM DESCRIPTION

The solar field AQUASOL-II (see Fig.1) located at the Plataforma Solar de Almería (PSA) in Spain, is composed of 60 stationary flat plate solar collectors (Wagner LBM 10HTF) with a total aperture area of 606 m^2. Its distribution is shown in Fig. 2. There are five loops connected in parallel: four of these loops (loops 2-5) have 14 flat-plate collectors each one (and each loop has two rows connected in series with 7 collectors in parallel per row) while loop 1 has 4 flat-plate collectors connected in parallel. There is a main pumping system (Pump 0) and each loop has its own pumping system (Pump 1-Pump 9). The main pump is required to help the others secondary ones reaching high flow levels.

Fig. 1. AQUASOL-II solar field facility at PSA (Spain).

As Fig. 2 shows, the water enters to the main pipe and it is pumped by the main pump through the loops. In loops 2-5 the water is pumped across the flat plate solar collectors by two pumping systems (the one on the left and the one on the right) and it flows to the main pipe to continues its cycle into the plant. From the control point

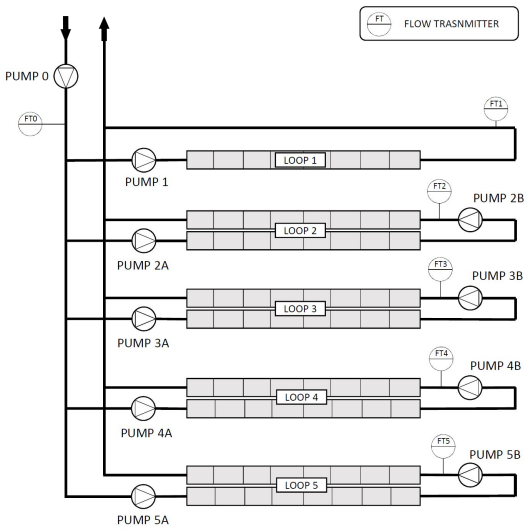

Fig. 2. Schematic diagram of AQUASOL-II solar field facility.

of view, the pumps inside each loop are treated as unique one. Therefore, the manipulated variable will be one for loop and each pump variable-frequency drive will receive the same value. It is important to mention that, during the experimental campaigns performed to obtain the model and test the controller, loop number 2 was out of order. For this reason, this loop is not considered neither in the modelling stage, nor in the control design.

III. HYDRAULIC MODEL

With the aim of tuning a controller to regulate the water flow rates inside the solar loops, an hydrualic model of the system has been obtained experimentally. Since the plant is a multiple-input multiple-output (MIMO) system with 5 inputs (pump speeds) and 5 outputs (water flow rates), the basic transfer function model is $\mathbf{y}(s) = \mathbf{G}(s)\mathbf{u}(s)$, where $\mathbf{y}$ and $\mathbf{u}$ are 5x1 vectors and $\mathbf{G}(s)$ is a 5x5 transfer function matrix. There is interaction between inputs and outputs because a change in one of the inputs affects all the outputs.

To obtain the values of matrix $\mathbf{G}(s)$, an experimental campaign was designed and performed; different steps were applied in the loops pumps to obtain the water flow rates responses via the reaction curve method. The experiments to find the data were planned as follows:

- The loops pumps (Pump 0, Pump 1, Pump 3a, Pump 3b, Pump 4a, Pump 4b, Pump 5a, Pump 5b) were characterized with steps from 40% to 90% of the input range.
- The experiments described in the previous bullet were repeated with different values in the principal pump (Pump 0) input. In particular, the principal pump was set to 20% 50% 80% of its input range.

In order to obtain a good data set, it was necessary to acquire the data when the water temperature was near to the operating point as the density of water changes according to its temperature. For that reason, it was necessary to make the experiments during a day with adequate solar radiation and the inlet temperature was controlled with an air-cooler located in the main pipe of the solar field. In order to use as less as possible the air-cooler, the experiment with the principal pump at 20% was done during the morning, when the solar radiation was not too high and the others in the afternoon. When required, the temperature of the water at the inlet of the solar field was maintained at 40°C using the air cooler.

A. GAIN

During the experimental campaign performed to obtain the transfer function models, it was observed that the static gain of the process changes with the operating conditions due to the nonlinearities of the actuators (pumps). In particular, the gain of the models of the loops pump depends on the working point of the main pump. This is reasonable because the energy losses in the pipe, as the Bernoulli equation states, depend on the square of the water speed.

This static nonlinearity is combined with transfer functions describing the linear part of the models, following the strategy described below:

1) plotting the experimental loops pump gains according to the pump 0 input signal;
2) interpolating the data with a polynomial;
3) considering two parts of the transfer function: one is a polynomial, p_{ij}, which defines the gain and the other is the linear dynamic part, G_{ij}.

Therefore, the water flow rate in each loop, y_i, where $i = 0$ is for the principal pump and $i = 1,3,4,5$ are for the loop i, is calculated as:

$$y_i = \sum_j y_{ij}, \quad i,j = 0,1,3,4,5, \tag{1}$$

where y_{ij} is the contribution to y_i due to the interaction between loop i and loop j, and they can be obtained from

$$\frac{Y_{ij}(s)}{U_{0j}(s)} = p_{ij}G_{ij}, \quad p_{ij} = f(u_0,u_j), \tag{2}$$

being p_{ij} the polynomial that defines the gain and that depends on the inputs of the main pump u_0, and of the pump of the other loops u_j.

The values obtained for p_{ij} and G_{ij} are included in Table II in the Appendix. Notice that those transfer functions that involve the main pump are first order transfer functions, while the dynamics between pumps of different loops must be defined with second order transfer functions.

1) MAIN PUMP: As shown in Eq. 2, to model the main pump's transfer function (pump 0), it is not necessary to introduce an additional input signal because the gain changes according only to the input u_0. Fig. 3 shows the experimental points obtained to evaluate the gain as a function of the principal pump input. In this case, it is possible to model this gain as a second order polynomial (see p_{00} in Table II).

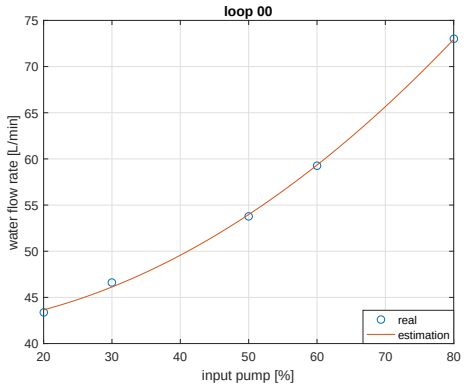

Fig. 3. Nonlinear gain obtained experimentally and the polynomial p_{00} curve fitting.

2) LOOPS PUMPS: The same procedure followed for the main pump was used to achieve the model's gain between the principal pump and each loop (polynomials p_{0j}, $j = 0,1,3,4,5$). These models are quite similar to the one shown above, but in the loops, the equation for the gain in the direct transfer functions (G_{ij}, being $i = j$) are first order polynomials and for the indirect ones (G_{ij}, being $i \neq j$) are second order polynomials.

B. DYNAMICS

The data collected to find out the model transfer function were analyzed with the Matlab System Identification toolbox. In order to find the correct transfer functions, it was necessary to remove the value of the operating point to get an incremental model. Since the signals of this hydraulic system do not present a significant noise, they were not filtered.

C. MODEL RESULTS

In Fig. 4 it is possible to see the similarities between the experimental data and the simulation results. In particular it is worth analyzing the model gain and dynamics. It can be observed that the steady state values reached in each loop for different values of the input reflect that the nonlinear gains are properly calculated to achieve the real values. Regarding the dynamics, it is possible to note that an acceptable tracking between the real flow and the simulation is obtained. Special attention should be given to the presence of positive zero which is distinctive of a non-minimum phase system. This implies that the MIMO PID controllers design is more challenging.

IV. MULTIVARIABLE CONTROLLER

In this solar field, each pump of the system influences all the system's pipes and not only the loop where it is located. Therefore, before designing the controller, the coupling and interactions between inputs and ouputs must be established. One methodology to evaluate the degree of interactions is the relative gain array (RGA) [7]. In this case, due to the nonlinearities, the RGA matrix is not constant, it depends on the operating point. Based on the experience at the facility, the principal pump uses to work at more than 50% of its speed. In order to follow as much as possible the real operation point, the RGA matrix was calculated when the pump 0 input is at 80%, obtaining the following one:

$$RGA_{80\%} = \begin{bmatrix} 21.24 & -5.38 & -5.27 & -4.32 & -5.27 \\ -5.32 & 8.11 & -0.63 & -0.50 & -0.66 \\ -5.34 & -0.61 & 8.43 & -0.62 & -0.86 \\ -4.22 & -0.51 & -0.72 & 7.26 & -0.82 \\ -5.35 & -0.61 & -0.82 & -0.82 & 8.61 \end{bmatrix}. \quad (3)$$

From the RGA matrix, it is clear that the input-ouput pairs must be stablished as y_i-u_i, with $i = 0,1,3,4,5$. As expected, the water flow rate in each loop must be controlled with the pumping system of that loop. With the aim of reducing the iteraction degree as much as possible, a decoupler has been included [5].

As described in Section III, this hydraulic system is a non linear system, so the MIMO controller includes some special features to deal with nonlinearities. To compensate these nonlinearities, the inverse of the pump characteristics can be placed after the lineal controller and before it is applied to the pump. As explained in [1], with this idea, it is possible to obtain a considerable improvement in the performance of the closed-loop system.

A. Principal pump

The principal pump does not directly control the flow in the loops but it is necessary to support the other pumps. For this reason it is controlled in *open loop*. In Fig. 5, the control scheme for the principal pump is shown. It is composed of three main blocks and the set-point is allocated as the sum of the set-points of each individual loop.

1) Lookup table 1: In this block a linear function obtained experimentally (see Eq. 4) receives the set-point SP_0, and provides a control signal u'_0. The control signal passes from 0% when the SP is also at 0, to 100% when the SP is set to *maximum flow* in a linear way:

$$u'_0 = 0.8333 \times (SP_0). \quad (4)$$

2) Lookup table 2: In order to compensate the nonlinearities of the system, a lookup table was used to calculate the control signal u_0. It is implemented as a piecewise linear function that approximates the inverse of the function that describes the gain of the model:

$$\begin{cases} u_0 = 2.91u'_0 - 106.34 & \text{if } u'_0 < 50\%, \\ u_0 = 1.68u'_0 - 44.75 & \text{if } u'_0 \geq 50\%. \end{cases} \quad (5)$$

3) Decoupling 0: In this block, the functions which are used for decoupling each loop are placed. These functions are not calculated in the ideal form because the transfer functions present delays and positive zeros. These positive zeros, with an ideal decoupling become positive poles that destabilise the system. Simplified decouplings are calculated as Eq. 6, where the first number indicates the loop pump and the second the

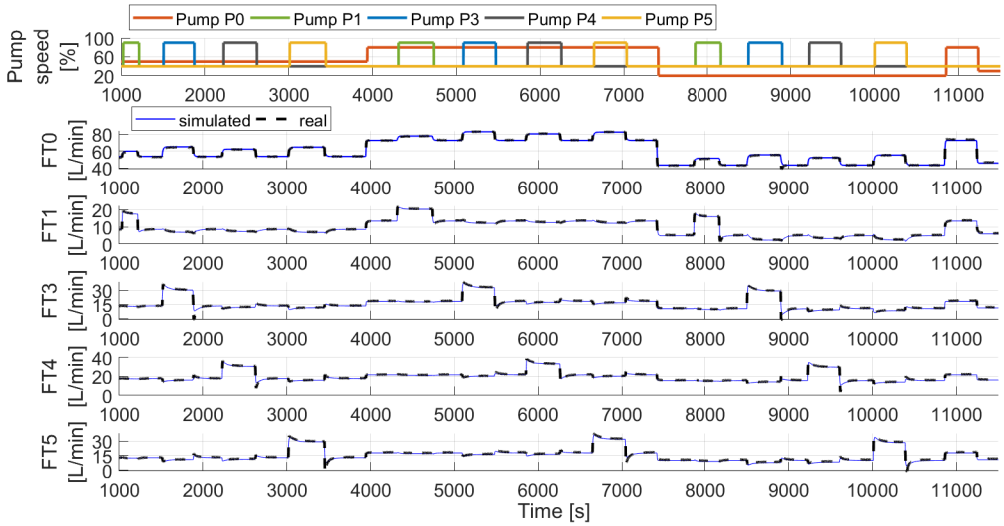

Fig. 4. Pumps speed (upper panel) and comparison between model results (blue solid line) and experimental data (black dashed line). Experimental test performed on March 15th, 2018.

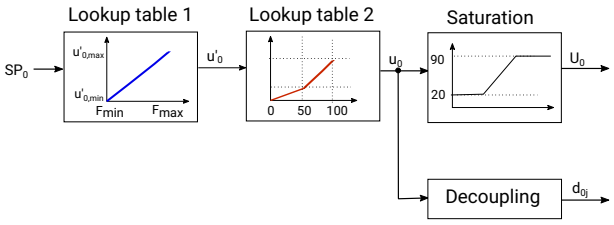

Fig. 5. Control structure for the principal pump.

affected loop. The D_{ij} transfer function in Eq. 6 are equal to the G_{ij} transfer function (see Tab. II) without delay.

$$R_{ij} = -\frac{D_{ij}}{D_{jj}} \quad i,j = 0,1,3,4,5. \tag{6}$$

B. Loop pumps

All the pumps on the loop are controlled with the same control scheme (see Fig. 6) and only the parameters change according to the model.

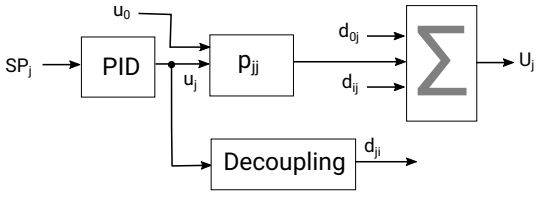

Fig. 6. Control structure for the loop j. Inputs from the main loop, u_0, d_{0j}, and from the other loops, d_{ij}, are required.

1) PID: this block implements a PID in the non-interactive form. Due to the presence of positive zeros, the derivative action is switched off.

2) Decoupling: the function in this block is calculated as described in Section IV-A.3.

3) MATLAB Function: This is the main difference between this control scheme and the tipical MIMO control structure. The signal from PID controller passes through this block which modifies the signal to compensate the nonlinearity. As it was said before, the nonlinear gain of each loop is connected with the principal flow. The following operations are performed in these blocks:

1) the value of the main flow is collected,
2) with that value the inverse of the model loop gain is calculated,
3) the signal coming from the PID controller is multiplied by the value obtained at the previous point and supplied at the output.

Due to the use of the *MATLAB Function* block, the gain of the system perceived by the PID controller in each moment is equal to one, then for the PID controller tuning it is necessary to consider a unitary gain. In this control scheme an *Anti-Windup* structure is also included because when the flow set-point is high the pump often achieves the saturation.

V. RESULTS

Different PID controller tunings were tested in simulation, being the best results obtained with the *Chien-Hrones-Reswick* rules [2], which are an improvement of the Ziegler-Nichols ones because they provide a higher robustness. This method provides different formulas for setpoint tracking and disturbance rejection and for 0% and 20% overshoot. In this case, the formulas for setpoint tracking and 20% overshoot have been used. As mentioned before, the derivative action was switched off because there is a positive zero in the system. Considering the parallel structure of the PI controller:

$$C(s) = K_p\left(1 + \frac{1}{T_i s}\right), \tag{7}$$

the obtained tuning is the one presented in Table I.

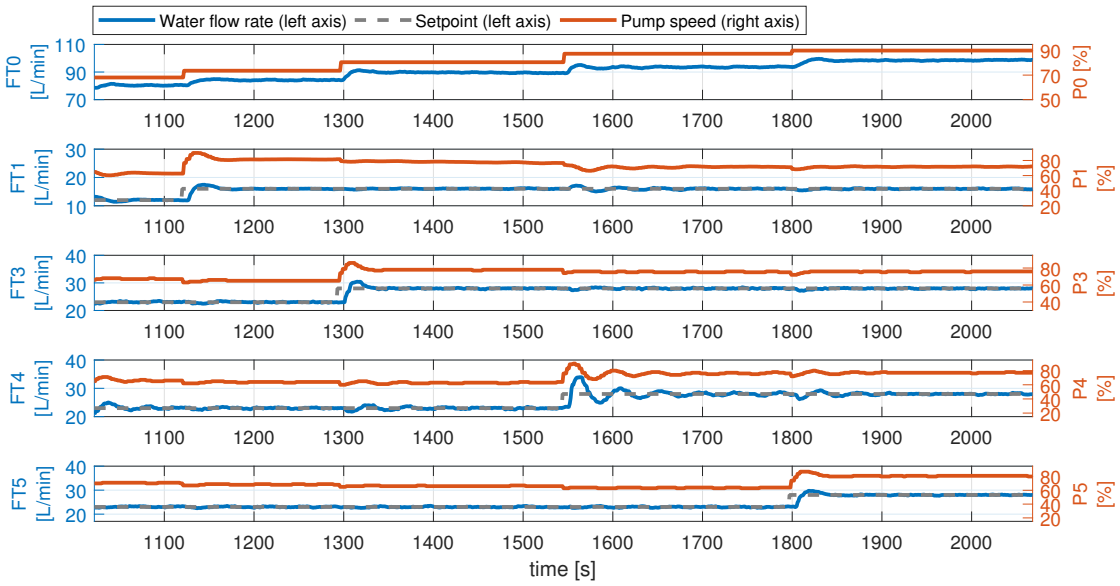

Fig. 7. Results obtained with the MIMO controller at AQUASOL-II facility (water flow rate in blue line and setpoint in grey dashed line are in the left axis, pumps speed in red line is in the right axis). Experimental test performed on March 31st, 2018.

PID Tuning	LOOP 1	LOOP 3	LOOP 4	LOOP 5
Kp (%L/min)	0.42	0.59	0.48	0.55
Ti (s)	4.24	4.90	3.17	4.57

TABLE I

PID TUNING OBTAINED FOR THE MIMO SOLAR FIELD SYSTEM

The proposed PID-based technique was tested on the real plant (see Fig. 7). The overshoot value is around 10% in the loops 1, 3, 5 and only in the loop 4 it reaches the 20%. Not all of these values are equal to 20% as the *Chien-Hrones-Reswick* rules said because of the model inaccuracy. According to what it was said about the overshoot, the oscillation is higher in the loop 4 while in the other loops are almost zero. The settling times of loops 1, 3 and 5 are less than one minute while loop 4 requires about two minutes to suppress the oscillation. These times are proper in order to control the temperature in the loops. The decoupling is not ideal so it is possible to see a small interaction between the loops but this interaction is indeed kept at an acceptable level.

CONCLUSIONS

In this paper we have shown that the flow in a solar collector system with a nonlinear MIMO dynamics can be effectively controlled by means of standard PID controllers by conditioning their output in order to compensate for the nonlinearities. An effective solution to condition the output is with a function that implements the inverse of the nonlinear part in order to linearize it. In this way the PID controllers see a linear system downstream.

This controller design is the first step to control the water temperature in the solar field. As the thermodynamics laws explain, the flow and the heat taken are connected and having an accurate flow control is an essential requirement in order to obtain a precise temperature control. In fact, the control structure presented in this paper will become the inner part of a *cascade control* where the master controller will calculate the required water flow rate in each loop to maintain a desired temperature at the outlet of the solar field. For this reason, a detailed study of the MIMO controller tuning must be performed; in particular, oscillations should be reduced (mainly in loop 4), but a fast response is also required for the cascade slave controller.

APPENDIX

Transfer functions and polynomials to calculate the gains of the hydraulic model are included in Table II.

REFERENCES

[1] K. J. Åström, and B. Wittenmark, Adaptive control. New York: Dover Publications, Inc, 2008.

[2] K. J. Åström, and T. Hägglund, PID controllers: theory, design, and tunning. Research Triangle Park, NC: Instrument Society of America, 1995.

[3] E. F. Camacho, M. Berenguel, F. R. Rubio, and D. Martínez, Control of solar energy systems. Springer Science & Business Media, 2012.

[4] J. D. Gil, L. Roca, G. Zaragoza, and M. Berenguel, A feedback control system with reference governor for a solar membrane distillation pilot facility, Renewable Energy, vol. 120, pp. 536-549, 2018.

[5] F. Morilla, J. Garrido, and F. Vázquez, Multivariable control by decoupling. Revista Iberoamericana de Automática e Informática industrial, vol. 10, pp. 3–17, 2013

[6] S. J. Navas, F. R. Rubio, P. Ollero, and J. M. Lemos. Optimal control applied to distributed solar collector fields with partial radiation. Solar Energy, vol. 159, pp. 811–819, 2018.

[7] S.Skogestad, and I. Postlethwaite, Multivariable feedback control: analysis and design. Chichester: John Wiley & Sons, 2001.

[8] J. Vergara-Dietrich, J. Normey-Rico, L. Roca, and M. Berenguel. Controle de temperatura em campos solares de grande porte utilizando a abordagem do PNMPC - Practical Nonlinear Model Predictive Control, presented at the XXI Congresso Brasileiro de Automática CBA-2016, Vitória, Brazil, 2016.

TABLE II

TRANSFER FUNCTIONS AND GAINS OF THE MIMO SYSTEM

	LOOP 0	LOOP 1	LOOP 3
P0	$G_{00}(s) = \frac{0.2464}{s+0.2464} e^{-4s}$ $p_{00} = 0.0048u_0^2 + 0.0073u_0 + 41.6$	$G_{10} = \frac{0.1351}{s+0.1351} e^{-4s}$ $p_{10} = 0.007u_0^2 + 0.0680u_0 + 3.6$	$G_{30} = \frac{0.4306}{s+0.4306} e^{-5s}$ $p_{30} = 0.0011u_0^2 + 0.0171u_0 + 10.5$
P1	$G_{01} = \frac{0.08997}{s^2+1.02s+0.08997} e^{-4s}$ $p_{01} = (8 \cdot 10^{-6}u_0^2 - 0.0018u_0 + 0.2) \cdot u_1$	$G_{11} = \frac{0.2946s+0.006409}{s^2+0.2628s+0.006409} e^{-6s}$ $p_{11} = (-0.0014u_0 + 0.2473) \cdot u_1$	$G_{31} = \frac{-0.2811s+0.008885}{s^2+0.4214s+0.008885} e^{-8s}$ $p_{31} = (-5.7 \cdot 10^{-6}u_0^2 + 7 \cdot 10^{-4}u_0 - 0.033) \cdot u_1$
P3	$G_{03} = \frac{2619}{s^2+2.675 \cdot 10^4 s+2619} e^{-4s}$ $p_{03} = (-4 \cdot 10^{-6}u_0^2 - 0.0003u_0 + 0.25) \cdot u_3$	$G_{13} = \frac{-0.101s+0.005787}{s^2+0.2839s+0.005787} e^{-5s}$ $p_{13} = (-8.2 \cdot 10^{-6}u_0^2 + 0.0013u_0 - 0.076) \cdot u_3$	$G_{33} = \frac{0.2895s+0.00306}{s^2+0.2189s+0.00306} e^{-5s}$ $p_{33} = (-0.0014u_0 + 0.4) \cdot u_3$
P4	$G_{04} = \frac{3334}{s^2+2.724 \cdot 10^4 s+3334} e^{-4s}$ $p_{04} = (-6.8 \cdot 10^{-6}u_0^2 + 0.0003u_0 + 0.17) \cdot u_4$	$G_{14} = \frac{-0.244s+0.01141}{s^2+0.588s+0.01141} e^{-5s}$ $p_{14} = (-2.6 \cdot 10^{-6}u_0^2 + 0.0005u_0 - 0.044) \cdot u_4$	$G_{34} = \frac{0.9392s+0.004963}{s^2+0.3571s+0.004963} e^{-4s}$ $p_{34} = (1.3 \cdot 10^{-6}u_0^2 - 3.4 \cdot 10^{-5}u_0 - 0.028) \cdot u_4$
P5	$G_{05} = \frac{0.04489}{s^2+0.5968s+0.04489} e^{-2s}$ $p_{05} = (-3.7 \cdot 10^{-6}u_0^2 - 0.0003u_0 + 0.25) \cdot u_5$	$G_{15} = \frac{-0.1333s+0.005995}{s^2+0.3164s+0.005995} e^{-3s}$ $p_{15} = (-5.8 \cdot 10^{-6}u_0^2 + 0.001u_0 - 0.07) \cdot u_5$	$G_{35} = \frac{0.4043s+0.003194}{s^2+0.1939s+0.003194} e^{-4s}$ $p_{35} = (2.8 \cdot 10^{-6}u_0^2 - 0.0001u_0 - 0.042) \cdot u_5$
	LOOP 4	LOOP 5	
P0	$G_{40} = \frac{0.4306}{s+0.4306} e^{-5s}$ $p_{40} = 0.001u_0^2 + 0.0031u_0 + 15.7$	$G_{50} = \frac{0.3748}{s+0.3748} e^{-5s}$ $p_{50} = 0.011u_0^2 + 0.022u_0 + 10$	
P1	$G_{41} = \frac{-0.2008s+0.007278}{s^2+0.4699s+0.007278} e^{-8s}$ $p_{41} = (-5.3 \cdot 10^{-6}u_0^2 + 0.0006u_0 - 0.026) \cdot u_1$	$G_{51} = \frac{-0.4016s+0.01599}{s^2+0.4264s+0.01599} e^{-8s}$ $p_{51} = (-6.2 \cdot 10^{-6}u_0^2 0.0007u_0 - 0.032) \cdot u_1$	
P3	$G_{43} = \frac{0.3592s+0.002649}{s^2+0.175s+0.002649} e^{-4s}$ $p_{43} = (5.6 \cdot 10^{-6}u_0^2 - 0.0005u_0 - 0.021) \cdot u_3$	$G_{53} = \frac{0.9557s+0.006807}{s^2+0.4268s+0.006807} e^{-8s}$ $p_{53} = (5.6 \cdot 10^{-7}u_0^2 + 0.0002u_0 - 0.048) \cdot u_3$	
P4	$G_{44} = \frac{0.4598s+0.005299}{s^2+0.3321s+0.005299} e^{-4s}$ $p_{44} = (-0.0008u_0 + 0.3) \cdot u_4$	$G_{54} = \frac{0.795s+0.005769}{s^2+0.35s+0.005769} e^{-4s}$ $p_{54} = (-4.9 \cdot 10^{-7}u_0^2 + 0.0001u_0 - 0.038) \cdot u_4$	
P5	$G_{45} = \frac{0.5236s+0.003655}{s^2+0.261s+0.003655} e^{-5s}$ $p_{45} = (3.2 \cdot 10^{-6}u_0^2 - 0.0003u_0 - 0.03) \cdot u_5$	$G_{55} = \frac{0.31s+0.0037}{s^2+0.2357s+0.0037} e^{-5s}$ $p_{55} = (-0.0014u_0 + 0.4) \cdot u_5$	